Hindawi
Shock and Vibration
Volume 2021, Article ID 7454596, 11 pages
https://doi.org/10.1155/2021/7454596

Research Article

A Case Study on the Deformation of Metro Foundation Pit in Silt Stratum in North China

Yonggang Zhang,[1] **Yonghong Wang**,[2] **and Yuanyuan Zhao**[3]

[1]*School of Civil Engineering, Beijing Jiaotong University, Beijing 100044, China*
[2]*Key Laboratory of Urban Underground Engineering, Ministry of Education, Beijing Jiaotong University, Beijing 100044, China*
[3]*School of Civil Engineering, Hebei University of Science and Technology, Shijiazhuang 050000, Hebei, China*

Correspondence should be addressed to Yuanyuan Zhao; zhaoyuanyuan@hebust.edu.cn

Received 27 July 2021; Accepted 24 September 2021; Published 28 October 2021

Academic Editor: Shan Gao

Geological conditions of urban subway foundation pits are controllable factors in determining the deformation of pits. In this paper, the monitoring data and statistical data of a subway deep foundation pit in North China are presented and compared with those of Tianjin subway. The deformation characteristics of the proposed pit, open excavated with triple-layer steel supports, are introduced in detail. Based on the aforementioned information, the energy conservation equation of the mobilized strength design (MSD) method in which the compression deformation energy of internal support is considered is applied to predict the maximum lateral movement. The maximum lateral movement turns out to be 22.2 mm according to the improved MSD method, which is very close to the measured value.

1. Introduction

In the construction of metro, the deformation control of deep pit is one of the most crucial topics. Excessive large deformation of the stratum will lead to the accidents of foundation pit and surrounding buildings. The deformation of foundation pit should be strictly controlled to reduce the impact of excavation on the surroundings.

Researchers and engineers have conducted extensive research on the deformation mode and failure mechanism of deep and large foundation pits, including the deformation prediction method of foundation pits and the estimation of ground settlement and horizontal displacement of wall.

Peck [1] conducted a detailed study on the ground settlement caused by the excavation of soft soil foundation pit and obtained the estimated value of the soil settlement outside the pit. Clough and O'Rourke [2] and O'Rourke [3] studied the deformation of the wall in the foundation pit of hard clay, residual soil, and sand. Wang et al. [4] and Yang and Lu [5], respectively, used numerical analysis methods to analyze the relationship between the deformation mode of support structure and the settlement range, settlement distribution form, the maximum value of settlement, and the location of the soil around the foundation pit. Wang et al. [6], Xu et al. [7,8], and Jiang et al. [9] collected the deformation data of Shanghai deep foundation pit engineering and discussed the deformation characteristics of foundation pit retaining structure from the statistical point of view.

In order to reduce the influence of deep foundation pit excavation on the surrounding environment, the deformation of supporting structure needs to be strictly controlled. In order to reflect the development of stress and displacement in the process of foundation pit deformation, Bolton et al. [10] proposed the design method of foundation pit retaining structure, namely, MSD (Mobilized Strength Design), based on the plastic deformation mechanism and virtual work principle. Bolton et al. [11, 12] and Osman and Bolton [13, 14] applied the MSD method to the cantilever deformation foundation pit of retaining wall. Wang et al. [15] introduced elastic strain energy of retaining wall to improve the MSD method. Liu et al. [16] introduced the influence of compression deformation energy of internal

support, bending deformation energy of retaining structure above excavation surface, and buried depth of excavation surface into energy conservation equation and proposed the curve form of variable wave peak cosine function. Xu et al. [17] proposed the improved MSD rigidity of the deep foundation pit support structure, which was verified in the support structure of the deep foundation pit of Nanjing Metro.

Based on the monitoring data of the deep foundation pit in a metro project of Shijiazhuang city in North China, this paper analyzes the deformation characteristics of the deep foundation pit under the condition of open excavation plus three steel supports, taking a two-story three-span box type underground frame structure station in Shijiazhuang city subway project as an example. The deep foundation pit project of Tianjin metro project which is located 260 km away from Shijiazhuang city in North China is used as a companion object. In the energy conservation equation of the MSD method, the compression deformation energy of internal support is introduced to predict the deformation characteristics of foundation pit and compared with the measured value.

2. Deformation Statistics of Metro Foundation Pit

2.1. Foundation Pit Retaining Structure. Shijiazhuang city is located in the Piedmont inclined plane, with a total terrain of 1.5~2.0‰ from west and northwest to east and southeast. The total length of the Metro Line 1 is 36.626 km where the first phase of the project is 23.9 km, with 20 underground stations and the average station spacing is about 1.2 km. Table 1 shows the basic information of the metro foundation pit. The strata in this area are artificial fill layer (Q^{ml}), Neogene sedimentary layer (Q_4^{al}), quaternary Holocene alluvial proluvial layer (Q_4^{al+pl}), and quaternary upper Pleistocene alluvial proluvial layer (Q_3^{al+pl}).

As shown in Figure 1, the excavation length of foundation pit in Shijiazhuang city is between 100 and 300 m, the width is between 20 and 45 m, and the length-width ratio is 8~14, among which the foundation pit with the length-width ratio of 10~12 accounts for 47.1%. In contrast, the ratio of length to width of the foundation pit of Tianjin Metro Line 6 is more evenly distributed than that of Shijiazhuang city Metro Line 1. The proportion of foundation pit with the ratio of length to width of 10~12 accounts for 12.2%. With the increase in the ratio of length to width, the proportion of foundation pit with open excavation method decreases.

The ratio between the depths of the retaining wall inserted into the pit bottom to the depth of the pit bottom is defined as the insertion ratio, which represents the soil condition of the area. The maximum insertion ratio of 17 metro stations in Metro Line 1 of Shijiazhuang city is 0.35 while the average insertion ratio is 0.21, as shown in Figure 2. Compared with Tianjin, the distribution is relatively concentrated. The insertion ratio in Metro Line 6 of Tianjin is obviously larger than that of Metro Line 1 of Shijiazhuang city. The maximum insertion ratio of Tianjin Metro is 1.15, the minimum is 0.62, and the average is 0.89. Moreover, when the depth of foundation pit is 20~25 m, the distribution of insertion ratio is relatively scattered.

2.2. Settlement of Foundation Pit. The maximum ground settlement behind the foundation retaining structures of Shijiazhuang city is shown in Figure 3. The maximum settlement is less than 40 mm, of which 15 30 mm accounts for 70%, and the distribution of each section is relatively uniform. The maximum ground settlement behind the foundation structures of Tianjin Metro is more than 40 mm, of which 30~40 mm accounts for 17.3%, far greater than that of Shijiazhuang city.

Figure 4 shows the distribution of the maximum lateral movement of foundation pit retaining structures of Shijiazhuang city metro. The largest lateral movement is between 10 mm and 24 mm, of which 14 mm to 18 mm accounts for 64.7%, while the proportion of lateral movement larger than 20 mm is very small, and the distribution is relatively concentrated. The maximum lateral movement of foundation pit retaining structures in Tianjin is between 10 mm and 40 mm, of which 30 mm to 40 mm accounts for 71.05%. It can be seen that the deformation of foundation pit of Shijiazhuang city subway is quite different from that of Tianjin subway. This reflects the leading role of geological conditions in the deformation of urban subway foundation pit.

3. Foundation Pit Condition of Representative Station No. 1

Station No. 1 in Metro Line 1 is an underground double deck island station, with a total length of 287 m, a standard section width of 21.1 m, a roof covering of 3.1 m, a standard section floor depth of 17.19 m, and a shield shaft section floor depth of 18.64 m. The main structure of the station is constructed by the open excavation method, and the structural type is the underground two-layer three-span box type frame structure. The average ground elevation within the construction scope of the station is 82.54 m, and the average covering soil thickness of the station structure is 3.1 m. The upper part of the main retaining structure of the station is the concrete retaining wall, while the lower part is the retaining pile plus steel support type. Three supports are installed in the open excavation standard section, as shown in Figure 5.

The stratum of the site is alluvial and diluvial stratum, and the lithology is quaternary Holocene cohesive soil and sand soil. There are collapsible loess like silt and loess like silty clay in the site. The self-weight collapsible amount is less than 70 mm; therefore, the collapsible type of the site is non-self-weight collapsible loess site (Table 2).

According to the mechanical properties, the foundation soil in the 55.00 m insertion depth range of station 1 can be divided into 10 sublayers, and the stratum profile and physical and mechanical properties of soil layer are shown in Figure 6.

When the insertion depth is less than 7.5 m and more than 17.5 m, the sensitivity of soil layer is lower ($S_t < 2$). The soil layer between 7.5 and 17.5 m is highly sensitive, which

Table 1: Basic information of the metro foundation pit.

	Length (m)	Width (m)	Length-width ratio	Pit depth (m)	Wall depth (m)	Insertion ratio
Max.	287.00	41.40	13.60	22.59	25.19	0.35
Min.	194.12	19.60	5.86	14.80	18.50	0.12
Average	230.36	22.78	10.36	17.28	21.15	0.23
Std.	24.15	4.80	1.63	1.85	1.93	0.05
CV	0.10	0.21	0.16	0.11	0.09	0.23

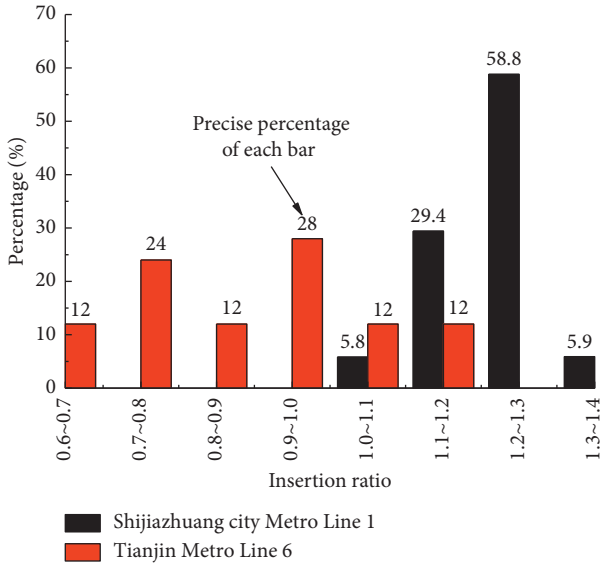

Figure 1: Length-width ratio distribution.

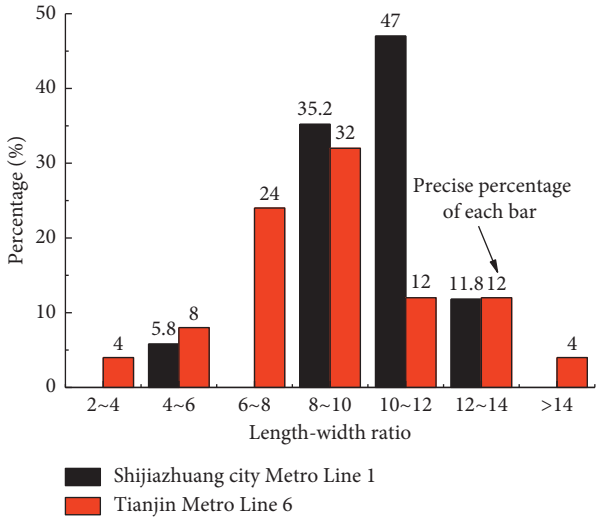

Figure 2: Insertion ratio distribution.

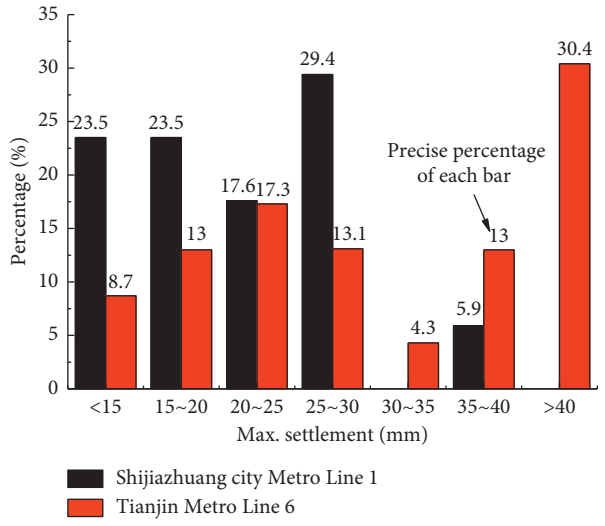

Figure 3: Distribution of maximum ground surface settlement behind retaining structures.

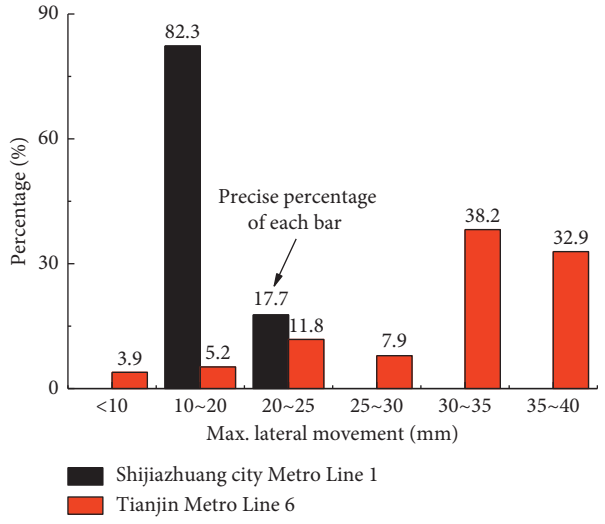

Figure 4: Distribution of maximum lateral movement of foundation pit retaining structures.

indicates that the strength and rigidity of soil in this range are easily disturbed by construction and significantly reduced.

From $0.1 < a_{s1\text{-}2} < 0.5$, it can be seen that within 55 m of the insertion depth, all are medium compressible soil. The shear strength indexes C_u and φ_u of soil are obtained from the direct shear test, for the stress-strain curve provided by the direct shear test which is closest to the in situ test results. It can be seen from the above parameters that the stratum of the foundation pit of Station No. 1 is medium hard clay, and its void ratio is less than 1. Due to the high compressibility of the stratum, the undrained shear strength is less than 75 kPa.

The triaxial test was carried out in the site field. The stress-strain curve of each layer is shown in Figure 7. The peak shear strength increases with the increase in insertion

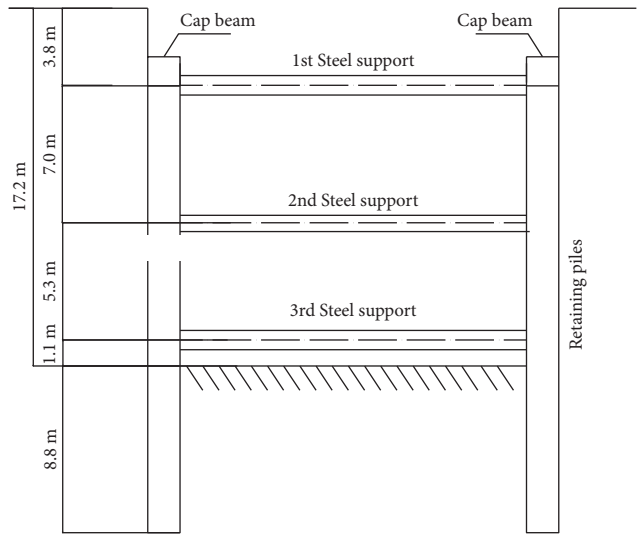

Figure 5: Retaining structures of Station No. 1.

Table 2: Feature of the stratum.

Stratum no.	Lithology	Density (g/cm^3)	Cohesion (kPa)	Friction angle (o)	Standard value of bearing capacity (kPa)	Static lateral pressure factor	Natural water content (%)
2-2	Loess silty clay	1.81	35	20	150	0.33	13.6
2-3	Loess silt	1.83	14	29	160	0.32	13.6
3-1	Loess silty clay	1.94	35	21	160	0.35	21.5
3-2	Loess silt	1.86	25	29	180	0.31	13.9
5-1	Silty clay	1.99	37	18	190	0.41	23.5
5-2	Silty soil	2.00	23	24	190	0.33	19.6
5-4	Medium coarse sand	2.03	0	31	200	0.30	—
6-3	Pebble	2.12	0	35	350	0.25	—

depth. In the nonyielding stage, with the increase in soil strain, there is a one-to-one relationship between stress and strain.

4. Deformation Analysis

4.1. Analysis of Deformation Monitoring Data. At the ends and middle point of the long side of the foundation pit, total 6 inclined holes for the retaining structure were evenly arranged to monitor the lateral movement curve at the depth of 15 m, as shown in Figure 8.

The foundation pit was constructed from the left end first, and the lateral movement of the retaining structure tended to be stable on May 18, 2014, lasting for 69 days; the final lateral movement was between 18 mm and 20 mm. The construction of the middle and right ends of the foundation pit started at the same time, and the lateral movement of the right end of the retaining structure tended to be stable on June 6, 2014, lasting 71 days; the final lateral movement was between 17 mm and 23 mm. The lateral movement of the retaining structure in the middle of the foundation pit tended to be stable on July 24, 2014, lasting for 118 days; the final lateral movement was between 18 mm and 20 mm, and the change gradient is relatively gentle.

The lateral movement duration curves of point M_{up} at the retaining structure are shown in Figure 9. The maximum lateral movement of the retaining structure occurs at the depth of 10 mm, while the minimum lateral movement occurs at the toe of the retaining structure.

There are 54 lateral movement monitoring points in the foundation pit. The relationship between the maximum lateral movement and the excavation depth is shown in Figure 10. It can be seen from the figure that the maximum lateral movement of the retaining structures is between 0.026%H and 0.240%H, with an average of 0.165%H (H is the excavation depth).

The relationship between the maximum lateral movement depth of the retaining structures and the excavation depth is shown in Figure 11. The maximum lateral movement depth of the retaining structures is between 7.5 m and 17.5 m, accounting for 90.17%. With the increase in excavation depth, the maximum lateral movement depth of the retaining structure tends to decrease whilst the distribution is more centralized, with an average depth of about 13 m, about 0.42H.

The ground surface settlement curves at 3 meters away from the retaining structures of the foundation pit are shown in Figure 12. It can be seen from the figure that behind the left lower side wall, the surface was uplifted; behind the

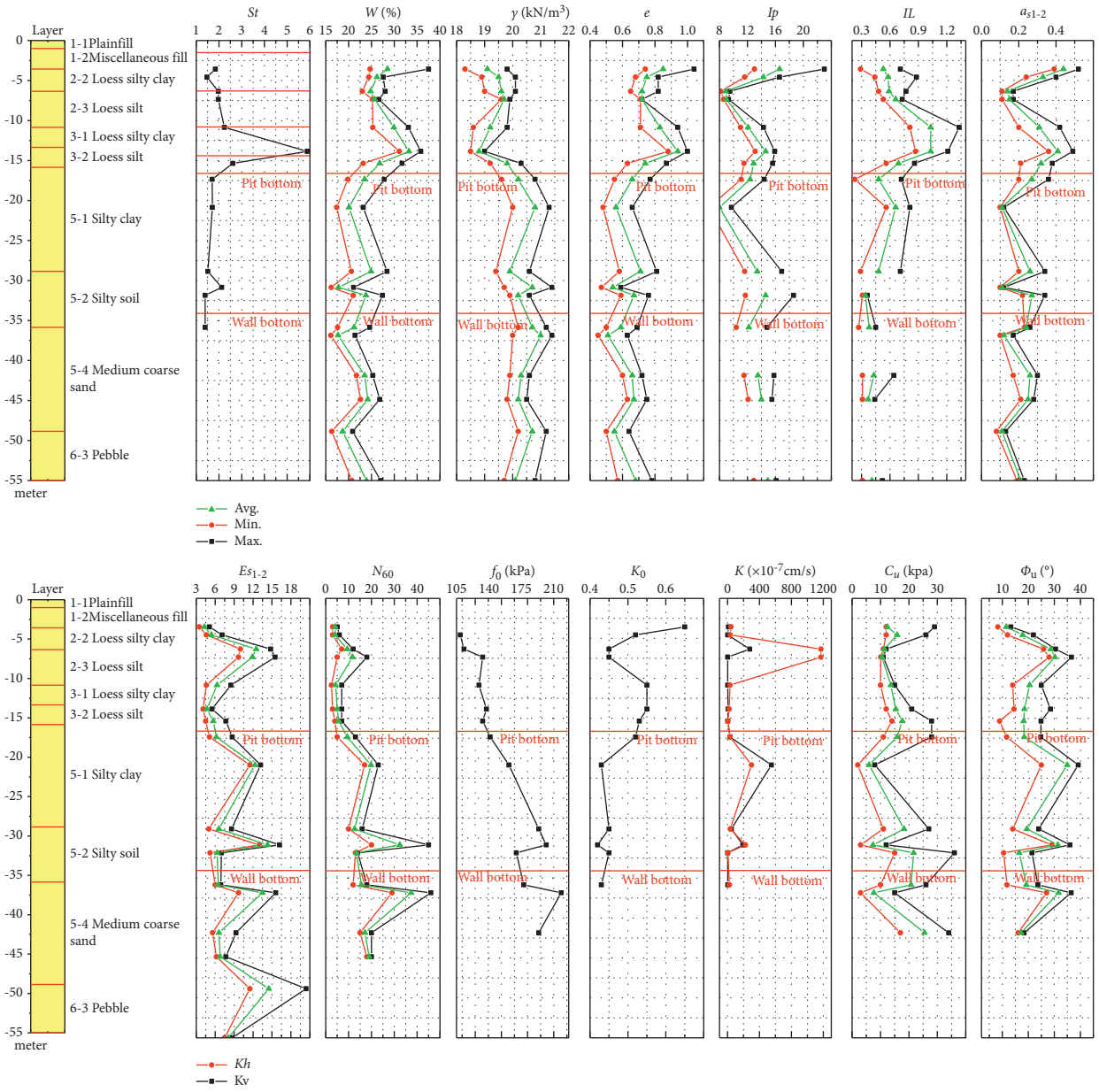

Figure 6: Physical and mechanical properties of soil layers.

middle lower side wall, the surface settlement was very small; and the maximum surface settlement behind the retaining structures was located at the right lower side wall, about 22 mm.

After excavation, the lateral movement of the retaining wall is shown in Figure 13. There is no obvious change rule of the lateral movement of the retaining wall. Due to the restraint of the internal support, the foundation pit does not show the characteristics of large deformation at the midpoint of the long side and small deformation at both sides, such as the cantilever foundation pit.

4.2. Improved Mobilized Strength Design. In this paper, the mobilized strength design (MSD) method, considering the compression deformation energy of the internal support, is used to to predict the maximum lateral movement of the retaining structures with following steps:

(1) Determine the soil stress-strain curve: collect the representative soil around the foundation pit for the indoor triaxial compression test and obtain the soil strength characteristic curve.

(2) Determine the cantilever type deformation: obtain the mobilization rate of undrained shear strength of soil through known parameters such as the buried depth of retaining structure, the excavation depth of foundation pit, and the weight of soil; obtain its undrained shear strain through the soil stress-strain curve; then obtain the deflection angle of the restaining wall and the maximum displacement of

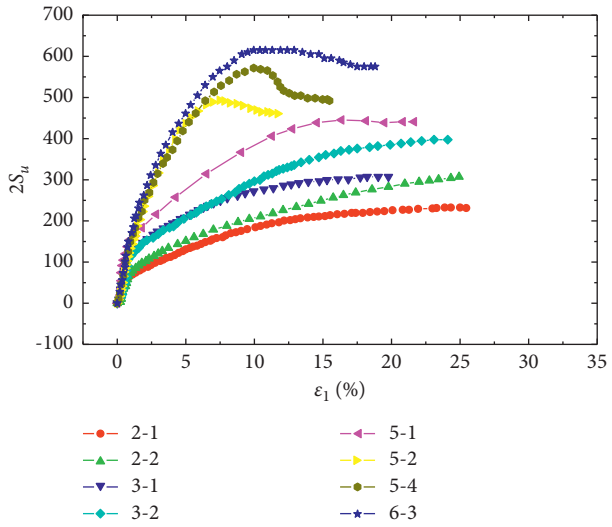

Figure 7: Stress-strain curves of the consolidated undrained triaxial test for each layer of soil.

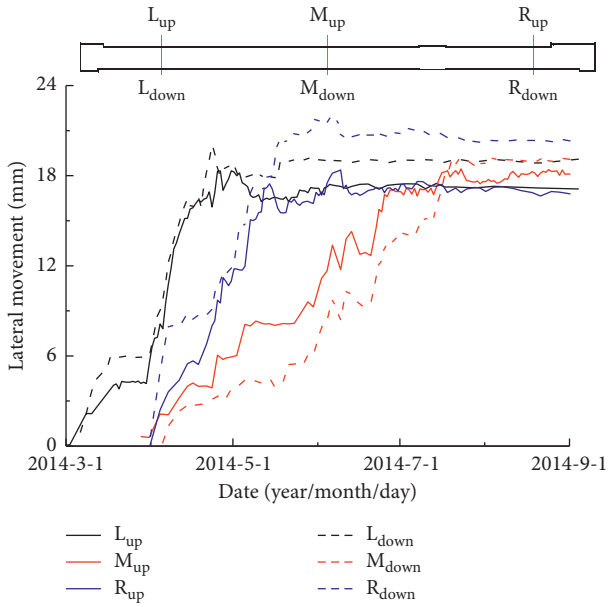

Figure 8: Lateral movement of retaining structures at the depth of 15 m.

wall top δ_{wm1}, as well as the cantilever type deformation curve:

$$\Delta_{w1}(y) = \Delta_{wm1} + \frac{\Delta_{wm1} y}{\lambda}; -\lambda \le y \le 0. \quad (1)$$

(3) Determine the excavation deformation in the second step: the influence wavelength of deformation is λ, and the excavation incremental deformation in the second step is approximated to the segment cosine function, namely:

$$\delta_{w2}(y) = \begin{cases} \frac{\delta_{wm2}}{2}\left[1 - \cos\left(\frac{\pi y}{k_2 \lambda}\right)\right]; -k_2\lambda \le y < 0 \\ \\ \frac{\delta_{wm2}}{2}\left[1 - \cos\left(\frac{\pi (y - (1-2k_2)\lambda)}{(1-k_2)\lambda}\right)\right]; -\lambda \le y < -k_2\lambda \end{cases} \quad (2)$$

In the second step, the total deformation curve is as follows:

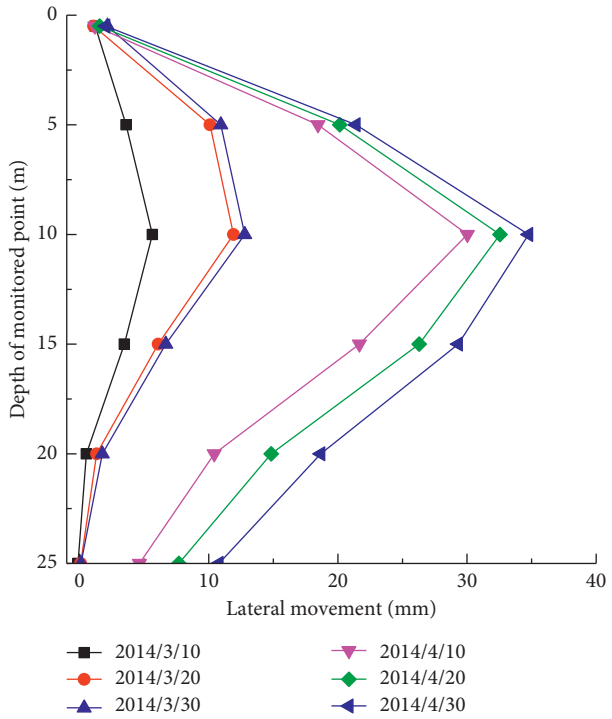

Figure 9: Lateral movement duration curves of point M_{up} at the retaining structures.

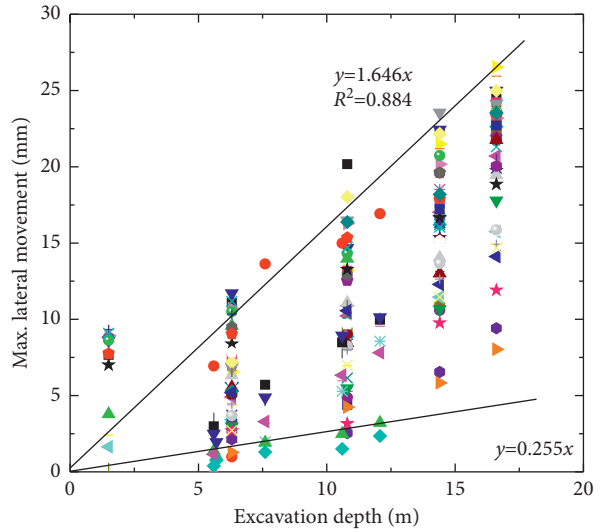

Figure 10: Relationship between the maximum lateral movement and the excavation depth.

$$\Delta_{w2}(y) = \begin{cases} \dfrac{\delta_{wm2}}{2}\left[1-\cos\left(\dfrac{\pi y}{k_2\lambda}\right)\right]+\left(\Delta_{wm1}+\dfrac{\Delta_{wm1}y}{\lambda}\right); & -k_2\lambda \le y < 0 \\ \dfrac{\delta_{wm2}}{2}\left[1-\cos\left(\dfrac{\pi\left(y-(1-2k_2)\lambda\right)}{(1-k_2)\lambda}\right)\right]+\left(\Delta_{wm1}+\dfrac{\Delta_{wm1}y}{\lambda}\right); & -\lambda \le y < -k_2\lambda \end{cases} \tag{3}$$

The derivative of $\Delta_{w2}(y)$ is as follows:

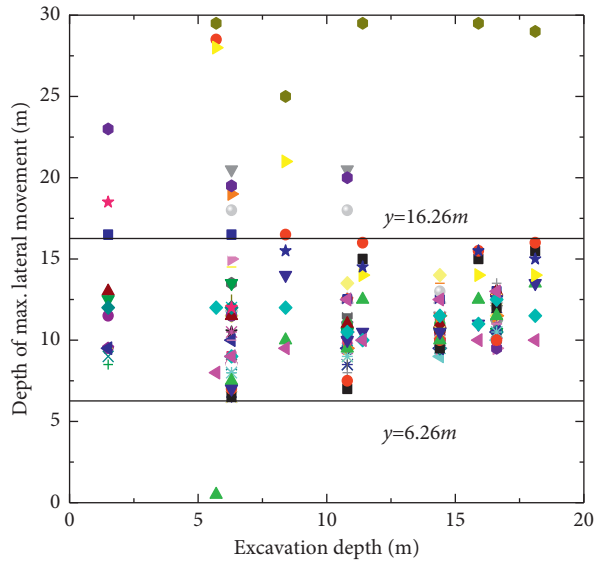

Figure 11: Relationship between the depth of the maximum lateral movement and excavation depth.

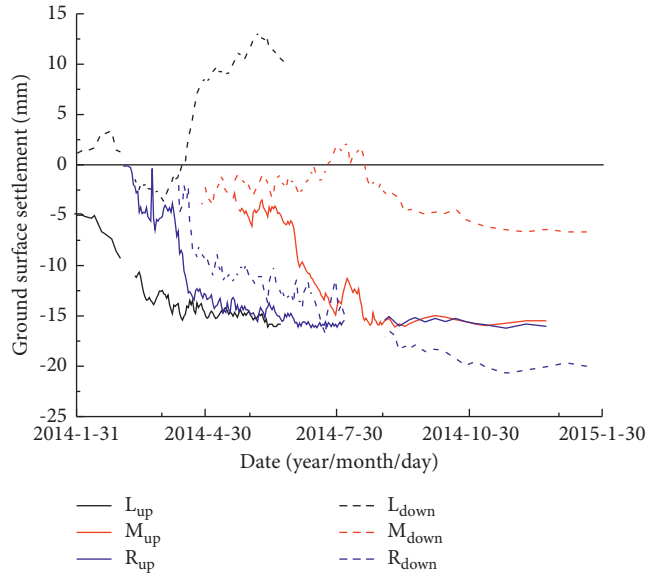

Figure 12: Ground surface settlement duration curves at 3 m distance from the retaining structures.

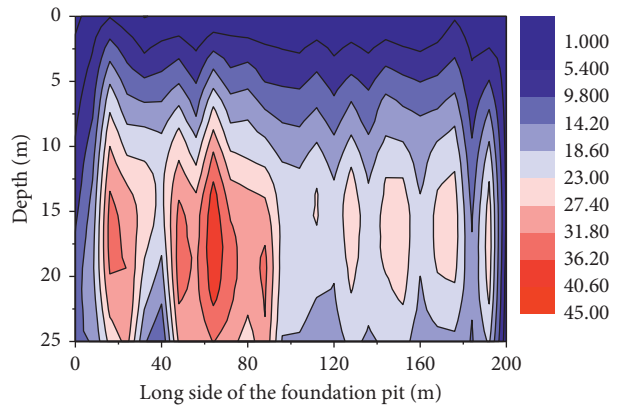

Figure 13: Lateral movement contour of the retaining structures after excavation.

$$\Delta'_{w2}(y)=\begin{cases}\dfrac{\delta_{wm2}}{2}\dfrac{\pi}{k_2\lambda}\sin\left(\dfrac{\pi y}{k_2\lambda}\right)+\dfrac{\Delta_{wm1}}{\lambda}; & -k_2\lambda\le y<0\\[2ex] \dfrac{\delta_{wm2}}{2}\dfrac{\pi}{(1-k_2)\lambda}\sin\left(\dfrac{\pi\left(y-(1-2k_2)\lambda\right)}{(1-k_2)\lambda}\right)+\dfrac{\Delta_{wm1}}{\lambda}; & \lambda\le y<-k_2\lambda\end{cases}\tag{4}$$

The value of the maximum lateral displacement of the retaining structure is the same as that of the excavation surface; then, when $y=H$, the value of $\Delta'_{w2}(y)=0$:

$$\begin{cases}\dfrac{\pi H}{k_2\lambda}\sin\left(\dfrac{\pi H}{k_2\lambda}\right)=-\dfrac{2\Delta_{wm1}}{\lambda\delta_{wm2}}H; & -k_2\lambda_2\le y<0\\[2ex] \dfrac{\pi\left(H-(1-2k_2)\lambda\right)}{(1-k_2)\lambda}\sin\left(\dfrac{\pi\left(H-(1-2k_2)\lambda\right)}{(1-k_2)\lambda}\right)=-\dfrac{2\Delta_{wm1}}{\lambda\delta_{wm2}}\left[H-(1-2k_2)\lambda_2\right]; & -\lambda_2\le y<-k_2\lambda_2\end{cases}\tag{5}$$

By equation (5), k_2 which makes the total deformation reach the maximum value can be obtained. The obtained k_2 is substituted into the incremental deformation curve, and the horizontal and vertical deformations of the soil mass on both sides of the foundation pit are calculated according to equations (4) and (5), and then the soil gravity potential energy ΔP expressed by δ_{wm2} is obtained.

When the width of the foundation pit $B<2[2(\lambda\text{-}h_0)]^{1/2}$, the foundation pit is a narrow foundation pit, and the influence range of the soil outside the pit is the same as that of the wide foundation pit. The influence range of the soil inside the pit is rectangular and obeys the two-dimensional shear state as follows:

$$\delta_y=\begin{cases}\dfrac{\lambda'\delta_m}{4B}\left(\pi+\dfrac{\pi y}{k\lambda'}-\sin\dfrac{\pi y}{k\lambda'}\right)\sin\left(\dfrac{\pi x}{B}\right); & 0\le y\le k\lambda',\\[2ex] \dfrac{\lambda'\delta_m}{4B}\left(\pi+\dfrac{\pi y}{(1-k)\lambda'}-\sin\dfrac{\pi y}{(1-k)\lambda'}\right)\sin\left(\dfrac{\pi x}{B}\right); & -(1-k)\lambda'\le y<0,\end{cases}\tag{6}$$

$$\delta_x=\begin{cases}\dfrac{\delta_m}{2}\left(1+\cos\dfrac{\pi y}{k\lambda'}\right)\cos\left(\dfrac{\pi x}{B}\right); & 0\le y\le k\lambda',\\[2ex] \dfrac{\delta_m}{2}\left(1+\cos\dfrac{\pi y}{(1-k)\lambda'}\right)\cos\left(\dfrac{\pi x}{B}\right); & -(1-k)\lambda'\le y<0,\end{cases}\tag{7}$$

According to the relationship between the maximum incremental deformation and the shear strain of the soil and the stress-strain curve of the soil, the internal energy ΔW consumed by the shear action of the soil expressed by δ_{wm2} is obtained. According to the flexural rigidity of the wall and the compressive rigidity of the internal support, the flexural deformation energy of the wall ΔU expressed by δ_{wm2} and the compressive deformation energy of the internal support ΔV are obtained. The external work produced by the self-weight of the soil behind the wall is equal to the internal energy dissipated by the shear action of the soil behind the wall and the strain energy produced by the bending deformation of the wall and the compression deformation of the support:

$$\begin{aligned}&\Delta P=\Delta W+\Delta U+\Delta V,\\ &\int_{\mathrm{vol}}\gamma_v\delta_v d\mathrm{vol}=\int_{\mathrm{vol}}c_{mob}\delta_\gamma d\mathrm{vol}+\frac{\mathrm{EI}}{2}\int_0^h\left[\frac{\mathrm{d}^2w_x}{\mathrm{d}y^2}\right]^2\mathrm{d}x\\ &\quad+\sum_{p=1}^{P}\frac{E_pA_p}{2l_p}\left(w_p\right)^2,\end{aligned}\tag{8}$$

where ΔP is the work done by external force; ΔW is the energy consumption of soil mass; ΔU is the elastic strain energy stored in the wall; ΔV is the elastic strain energy stored in the support; γ_v is the unit volume weight of soil mass; δ_v is the vertical displacement of soil mass behind the wall; c_{mob} is the mobilization value of soil strength; δ_γ is the

Table 3: The energy increment of each step.

Items	Construction steps			
	2	3	4	5
ΔP (J/m)	4.21	9.425	38.745	53.82
ΔW (J/m)	3.95	9.005	35.24	52.775
ΔU (J/m)	0.26	0.06	0.075	0.035
ΔV (J/m)	0	0.365	3.43	1.01
ΔU/ΔP (%)	3.09	0.32	0.095	0.035
ΔV/ΔP (%)	0	1.935	4.425	0.94

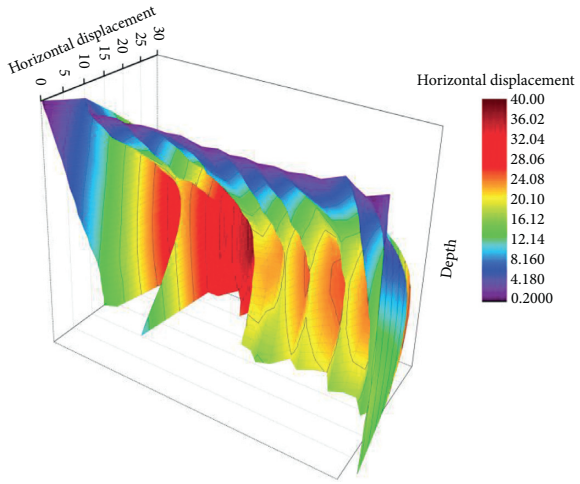

Figure 14: Horizontal displacement of the retaining wall.

increment of shear strain; EI is the elastic modulus of retaining wall; dw_x is the increment of horizontal deformation of retaining structure along the wall depth; h is the depth of retaining wall; F_s is the supporting axial force; l is the supporting length; and EA is the tensile rigidity of the member.

According to Equation (6), the maximum lateral displacement value δ_{wm2} of the wall is obtained, and whether it meets the design standard is judged, and the parameters are adjusted until the satisfactory result is obtained. The solution δ_{wm2} is substituted into Equation (3) to get the deformation curve of the second excavation step.

4.3. Validation of Improved MSD. In the proposed pit, the intermediate pile, bored pile, and internal corner reinforcement were constructed as Step 1. From Step 2 to Step 4, the proposed pit was excavated layer by layer, each time 0.5 m below the steel support. In Step 5, the pit was totally excavated. Table 3 gives the energy parameters calculated by the improved MSD method where ΔP is the work done by external force; ΔW is the energy consumption of soil mass; ΔU is the elastic strain energy stored in the wall; and ΔV is the elastic strain energy stored in the support. Horizontal displacement of retaining wall is shown in Figure 14. Vertical displacement of surface behind the wall is shown in Figure 15.

According to the improved MSD method in this section, the lateral movement curves of the wall are compared with

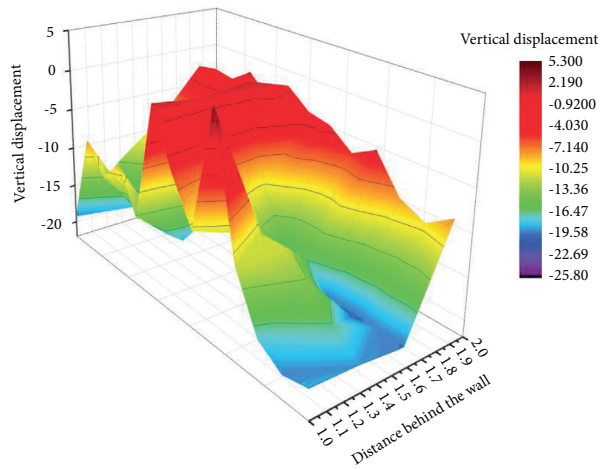

Figure 15: Vertical displacement of the surface behind the wall.

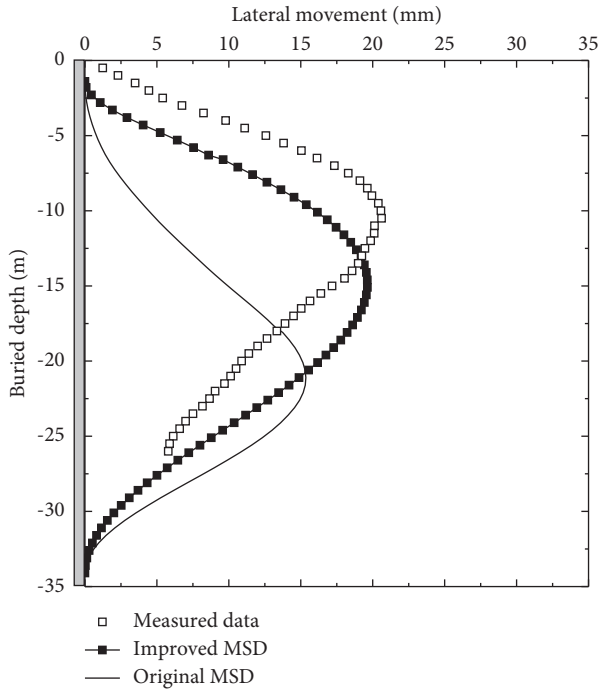

Figure 16: Comparison of measured data and calculated values.

the original MSD method and the measured data, as shown in Figure 16. It can be seen that the deformation curves obtained by the improved MSD are closer to the measured data than the original MSD method. In the proposed pit, the maximum lateral movement $\delta_{hm} = 23.4$ mm and the corresponding buried depth $H_{\delta hm} = 7.0$ m. It is predicted by the improved MSD method that $\delta_{hm} = 22.2$ mm and $H_{\delta hm} = 10.1$ m, while $\delta_{hm} = 17.4$ mm and $H_{\delta hm} = 14.1$ m according to the original MSD method.

5. Conclusions

(1) The average insertion ratio in Tianjin Metro is 0.89, which is significantly greater than that in Shijiazhuang city; the maximum lateral movement of

the foundation pit in Tianjin Metro is between 30 mm and 40 mm, while the maximum lateral movement of the wall is between 14 mm and 18 mm in Shijiazhuang city.

(2) In the proposed pit, the maximum lateral movement of the wall is about 0.165%H; the maximum lateral movement buried depth is between 7.5 m and 17.5 m.

(3) The compression deformation energy of internal support is considered in the energy conservation equation of the MSD method, and the maximum lateral movement $\delta_{hm} = 22.2$ mm, and the corresponding buried depth $H_{\delta hm} = 10.1$ m while $\delta_{hm} = 17.4$ mm and $H_{\delta hm} = 14.1$ m according to the original MSD method. In the proposed pit, $\delta_{hm} = 23.4$ mm and $H_{\delta hm} = 7.0$ m, the improved MSD method is more acceptable than the original MSD method.

Data Availability

The data used to support the findings of this study are included within the article.

Conflicts of Interest

The authors declare that there are no conflicts of interest.

Acknowledgments

This project was supported by the National Natural Science Foundation of China (51478037), which is gratefully acknowledged.

References

[1] R. B. Peck, "Deep excavation and tunneling in soft ground," in *Proceedings of the 7th International Conference on Soil Mechanics and Foundation Engineering*, pp. 225–290, State-of-the-Art-Volume, Mexico City, 1969.

[2] G. W. Clough and T. D. O'Rourke, "Construction induced movements of in situ wall," in *Proceedings of the ASCE Conference on Design and Performance of Earth Retaining Structures*, pp. 439–470, Geotechnical Special Publication No. 25, ASCE, New York, 1990.

[3] T. D. O´Rourke, "Base stability and ground movement prediction for excavations in soft clay. Retaining-structures," in *Proceedings of the International Conference on Retaining Structures*, pp. 657–686, Tomas Telford, London, July 1993.

[4] J. H. Wang, Z. H. Xu, and W. D. Wang, "Analysis of deformation behavior of deep excavations supported," *Chinese Journal of Geotechnical Engineering*, vol. 29, no. 12, pp. 1899–1903, 2007.

[5] M. Yang and J. Y. Lu, "Estimation of ground settlement aroused by deep excavation," *Chinese Journal of Geotechnical Engineering*, vol. 32, no. 12, pp. 1821–1828, 2010.

[6] B. J. Wang, J. H. Xiong, and B. T. Zhu, "Influence of deformation modes of retaining structures on surface settlements," *Structural Engineers*, vol. 23, no. 3, pp. 47–52, 2007.

[7] Z. H. Xu, J. H. Wang, and W. D. Wang, "Deformation behavior of diaphragm walls in deep excavations in Shanghai," *China Civil Engineering Journal*, vol. 41, no. 8, pp. 89–94, 2008.

[8] Z. H. Xu, J. H. Wang, and W. D. Wang, "Deformation behavior of excavations retained by bored pile wall in soft soil," *Rock and Soil Mechanics*, vol. 30, no. 5, pp. 165–169, 2009.

[9] X. F. Jiang, G. B. Liu, W. L. Zhang, and X. Y. Li, "Deformation characteristics of ultra-deep foundation pit in Shanghai based on measured data," *Chinese Journal of Geotechnical Engineering*, vol. 32, no. S2, pp. 570–573, 2010.

[10] M. D. Bolton, S.-Y. Lam, P. J. Vardanega, C. W. W. Ng, and X. Ma, "Ground movements due to deep excavations in Shanghai: design charts," *Frontiers of Structural and Civil Engineering*, vol. 8, no. 3, pp. 201–236, 2014.

[11] M. D. Bolton, W. Powrie, and I. F. Symons, "The design of stiff in-situ walls retaining over-consolidated clay part 1, short term behavior," *Ground Engineering*, vol. 23, no. 1, pp. 34–39, 1989.

[12] M. D. Bolton, W. Powrie, and I. F. Symons, "The design of stiff in-situ walls retaining over-consolidated clay part 2, long term behavior," *Ground Engineering*, vol. 23, no. 2, pp. 22–28, 1990.

[13] A. S. Osman and M. D. Bolton, "A new design method for retaining walls in clay," *Canadian Geotechnical Journal*, vol. 41, no. 3, pp. 451–466, 2004.

[14] A. S. Osman and M. D. Bolton, "Ground movement predictions for braced excavations in undrained clay," *Journal of Geotechnical and Geoenvironmental Engineering*, vol. 132, no. 4, pp. 465–477, 2006.

[15] H. R. Wang, W. D. Wang, M. S. Huang, and Z. H. Xu, "Modified mobilizable strength design (MSD) method on deformation predictions of foundation pit," *Chinese Journal of Rock Mechanics and Engineering*, vol. 30, no. S1, pp. 3245–3251, 2011.

[16] M. L. Liu, Q. Fang, D. L. Zhang, and Y. J. Hou, "Prediction of transient deformation due to excavation based on improved MSD method," *Chinese Journal of Rock Mechanics and Engineering*, vol. 37, no. 7, pp. 1700–1707, 2018.

[17] H. Z. Xu, P. P. Sun, W. S. Cui, and Y. J. Sun, "MSD synthetic system stiffness and deformation prediction of support structure for deep excavation in Nanjing subway," *Journal of China University of Mining & Technology*, vol. 47, no. 4, pp. 907–912, 2018.